Influence of rheological characteristics on the morphology of chemically-foamed biobased polymers by single-screw extrusion

Clément Duborper, Cédric Samuel, Cyril Loux, Marie-France Lacrampe, Patricia Krawczak

Influence of Rheological Characteristics on the Morphology of Chemically-Foamed Biobased Polymers by Single-Screw Extrusion

Duborper C.[1,2], Samuel C.[1], Loux C. [1], Lacrampe M.F.[1], Krawczak P.[1]

[1]*Mines Douai, Department of Polymer and Composite Technology & Mechanical Engineering (TPCIM), 941 rue Charles Bourseul, CS 10838, F-59508 Douai, France*

[2]*French Institute for Biobased Materials (IFMAS), 60 avenue Halley, F-59650 Villeneuve d'Ascq, France*

Abstract. This paper addresses the influence of the polymer rheology on cell nucleation and growth in biobased poly(butylene succinate) (PBS) foams produced by single-screw extrusion in the presence of an endothermic blowing agent. Various poly(ethylene) (PE) grades were also tested as model materials. Foam morphologies were observed and characterized by scanning electron microscopy followed and image analysis. Similar foam densities are obtained around 0.4 g/cm^3 and the cell density can be tuned between 5.10^4 and $1.4.10^5$ cells/cm^3. Based on polymer melt rheology and nucleation theories, the relationship between experimental cell density and simulated pressure profiles in the die computed using a commercial finite element software package were discussed. Low-density PE with branched architectures tends to favor a uniform cell size thanks to strain-hardening phenomenon. Thus, an accurate control of the foam morphology seems possible by tuning the polymer macromolecular architecture. An extrapolation of this result was made to three PBS commercial grades. The PBS grade with the highest melt viscosity and crystallization rate is the only one displaying promising features in terms of cell density and cell size. Consequently, the development of foamable PBS grades with tailored morphologies still requires extensive modifications of macromolecular architectures and precise tuning of rheological parameters to meet the requirements of number of industrial applications and enlarge the accessible markets.

Keywords: Processing, Extrusion, Foaming, Morphology, Simulation, Biobased polyesters, Sustainable plastics

INTRODUCTION

Polyurethanes and polystyrene foams were historically developed for thermal isolation and mechanical absorption in packaging; in such applications, there is no need to accurately control the foam morphology, which is characterized by heterogeneous cell sizes (ranging from 200 µm and 1 mm) (Chaur-Kie et al. 2005, Müller et al. 2005). Nowadays, there is an ever-growing interest in using plastic foams in engineering and therefore more demanding applications, and especially for automotive and medical markets where lightweight and functional materials with high mechanical strength and/or rigidity are required (Lee & Sha 2005, Gomes et al. 2001). As a consequence, advanced applications of polymer foams specifically require an accurate tailoring and control of the foam morphology in terms of cell density, cell size and cell distribution.

Poly(ethylene) (PE), poly(propylene) (PP), poly(carbonate) (PC), acrylonitrile-butadiene-styrene (ABS) foams were extruded using either chemical or physical foaming agents (Okolieocha et al. 2015). Homogeneous foams with cell size ranging from 1 and 100 µm could be produced this way and a relationship has been pointed out between the polymer rheology at melt state and the resulting foam morphology. In case of chemically-foamed plastics, the chemical blowing agent is decomposed into various gases (nitrogen, water, carbon dioxide) and a homogenous gas/polymer mixture is formed at high pressure. Then, a pressure drop is applied to polymer/gas mixture and the pressure drop rate becomes a key driver of the cell density, in accordance with several nucleation theories of the homogenous and heterogeneous nucleation (Van Stralen 1966, Lee et al. 2007). Several authors also identify a major effect of the elongational viscosity, with a marked strain-hardening, on the cell size homogeneity of polymer foams produced by extrusion.

Besides, the use of biobased polymers made from renewable raw materials attracts much attention due to their environmental friendliness and potential (bio)-degradability. Several biobased polymers display promising physical properties, and among them especially poly(butylene succinate) (PBS) with melting temperature (approx. 120°C) and mechanical properties close to PE (Wang et al. 2011). Among biobased polymers, only poly(L-Lactide) (PLA) and starch-based plastics were successfully foamed by extrusion technologies with a moderate control over the

foamed morphologies (Julien et al. 2012, Julien et al. 2015, Willet & Shogren 2002). To the best of our knowledge, the foaming ability of PBS was not investigated.

Therefore, the present work aims at identifing the influence of polymer rheology on the morphology of PBS plastic foams produced by single-screw extrusion with an endothermic chemical blowing agent. At first, various linear and branched low-density poly(ethylene), chosen as model materials, will be investigated to highlight key parameters controlling the cell density, cell size and uniformity. The influence of the pressure drop rate/residence time will be considered based on numerical simulations. Then, the results will be extended and extrapolated to biobased PBS. Finally, further guidelines to develop new foamable PBS grades will be discussed.

EXPERIMENTALS

Materials

The polymers investigated in the present work are: two low-density poly(ethylene) (LDPE - Riblene® MR10 from Polimeri Europa and Exceed 2018CA from Exxonmobil, hereafter respectively called PE1 and PE2); one linear low-density polyethylene (LLDPE - Flexirene CL10 from Polimeri Europa, hereafter called PE3); one modified linear low-density polyethylene (LLDPE - Bodyram 4108 from Polyram, hereafter called PE4); and two PBS grades (Bionolle 1903MD from Showa Denko and GSPLA FZ91PD from Mitsubishi, hereafter respectively called PBS1 and PBS2). The endothermic chemical foaming agent (CFA) is a masterbatch (Hydrocerol® ITP848 from Clariant) having a degradation temperature between 130 and 250°C. The CFA was dry-blended with polymer pellets at a concentration of 2% by weight prior to extrusion.

Processing and numerical simulations

A single-screw extruder (Kaufmann, screw length 840 mm, screw diameter 30 mm) was equipped with a static mixer and specific cylindrical 4-exit die (**Figure 1)**. Temperatures were set to 120, 160 and 190°C from the hopper the end of the extruder barrel, followed by 140 °C at the static mixer and 110°C at the die. Foams were produced at a screw speed of 60 rpm for a mass flow rate ranging between 100 and 200 g/min depending on the polymer grade. The melt temperature (approx. 130°C) and pressure were measured at the die entrance using a thermocouple/pressure sensor. For numerical simulations, the die geometry was reproduced within the commercial finite element Comsol Multiphysics® 5.1software package. The Navier-Stokes/heat transfer equations were then solved on the basis of the entrance pressure.

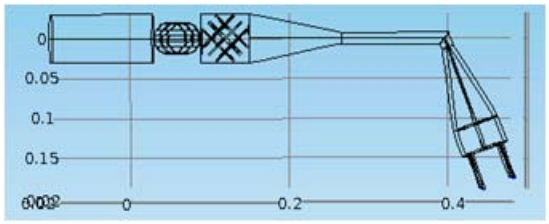

Figure 1: Schematic representation of the static mixer – die system

Characterizations

Oscillatory shear measurements were performed using an advanced rheometric system (Haake Mars III, ThermoScientific). Samples were equilibrated at desired temperature (ranging from 130 to 190°C) for 10 min before testing. The measurements were performed under nitrogen atmosphere using plate and plate geometry (diameter 35 mm, gap 2mm) with frequency sweep from 100 to 0.2 rad.s^{-1} within the linear domain of the materials.

The expansion ratio (τ) is determined as the D/D_0 ratio, where D and D_0 are the diameter of the expanded sample and the diameter of the sample extruded without expansion agent respectively. The cellular morphology of the transverse cross section of the extruded samples, previously coated with a thin gold layer (Polaron E5100 series II, Watford), was observed under high vacuum with a Scanning Electron Microscope (SEM, S-4300SE/N, Hitachi) operating at 5 kV, with a magnification of 35. The SEM pictures were analyzed a using an image processing software (ImageJ). Using all the cells through the cross section, the number average cell diameter in number (d_n), the volume average cell diameter in volume (d_v), the cell diameter polydispersity (I_D) and the cell density (C) were calculated by **equations 1-4**.

$$Dn = 2 * \frac{\sum ni * Ri}{\sum ni} \quad \textbf{(Eq. 1)}; \qquad Dv = 2 * \frac{\sum ni * Ri^4}{\sum ni * Ri^3} \quad \textbf{(Eq. 2)}; \qquad I_D = \frac{dv}{dn} \quad \textbf{(Eq. 3)}$$

$$\mathcal{C} = \frac{1}{1-\varphi} * \left(\frac{n*M^2}{Am}\right)^{3/2} \textbf{(Eq. 4)},$$

with n_i the number of cell having a radius of R_i, n the total cell number, A_m the area of the extruded part (cm^2), M the magnification coefficient of the microscope and φ the void fraction of the sample.

RESULTS & DISCUSSION

At first, the various poly(ethylene)s with MFI values ranging from 1 to 20 (g/10min at 210°C) were investigated. A specific attention was paid to the influence of the melt rheology on the morphology of polymer foams manufactured by extrusion. The low-density PE and linear low-density PE were especially chosen to observe the effect of the long chain branching together with the melt viscosity. All PE were foamed in the same extrusion conditions. In a first approach, similar densities are obtained close to 0.4 g/cm^3 for all foamed samples, representing about 50% decrease of the initial density (**Table 1**). In the same time, the expansion ratio could be tuned between 52% and 15% compared to the neat sample. To get a deeper insight on the cell structure, cross sectional morphology of cylindrical expanded samples were observed by SEM (**Figure 2**). Extrusion foaming of PE only produces closed-cell foams and significant differences are observed between all samples in terms of cell size and cell density. After image analysis, cell size, cell uniformity and cell density were evaluated (**Table 1 – Equations 1-4**). The cell size D_n and D_v could be tuned between 160 and 530 µm with respect to PE grade, whereas the cell density could be adjusted between 5 and 14.10^4 $cells/cm^3$.

Table 1: Foam density, expansion ratio, cell size, uniformity and cell density for PE foams.

Material	ρ_{foam} (g/cm^3)	τ (%)	D_v (µm)	D_n (µm)	I_D	Cell density (10^4.cells/cm^3)
PE1	0.42	52	530	380	1.4	8.3
PE2	0.46	22	270	160	1.7	14.0
PE3	0.44	14	420	200	2.0	5.1
PE4	0.43	15	450	170	2.4	13.8

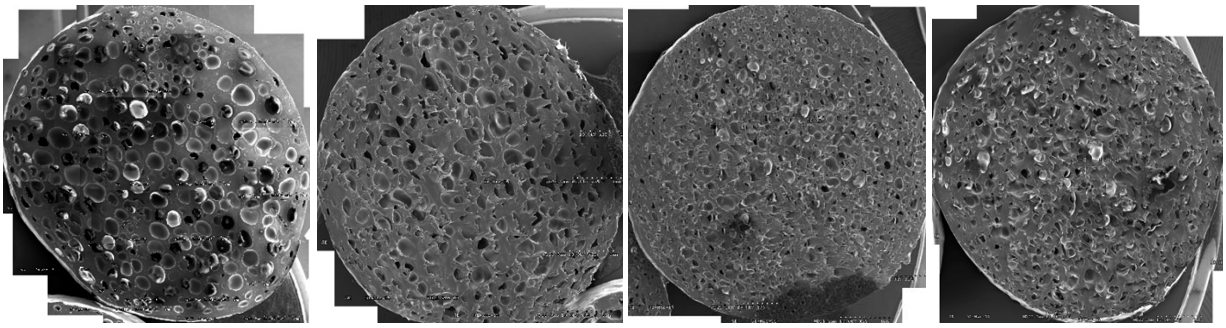

Figure 2: Morphologys of PE1, PE2, PE3 and PE4 foams (from left to right) as observed by scanning electron microscopy.

Then, the establishment of correlations with the melt rheology was attempted. Oscillatory-shear experiments were performed at melt state. The melt temperature and the shear rate were about 130°C and 300 s^{-1} in the die. In these conditions, complex viscosities η* of 570, 2930, 3630 and 5200 Pa.s are obtained from dynamic rheology measurements for PE1, PE3, PE4 and PE2 respectively. In this respect, one can state out that the cell diameter is primarily governed by the viscosity of the melt (**Table 1**). Low-viscosity polymers tend to generate higher cell size, and a certain level of control over the cell size is possible according to the melt viscosity of polymer. However, regarding cell size uniformity, only low-density PE (PE1 and PE2) are characterized by a low dispersity value (lower than 1.7) whereas linear low-density PE are systematically marked by high cell size dispersity (higher than 2). The macromolecular architecture, and especially long-chain branching with subsequent viscosity strain-

hardening in extensional flows, seems to play a major role on the uniformity via a stabilization effect as observed on PP foams (Spitael & Macosko 2004).

Concerning the cell density, an opposite trend to cell size tends to be observed; however only a rough correlation is obtained. Homogeneous cell nucleation theory predicts that the nucleation rate (or the number of cell produced per time unit) depends on various physical parameters such as the polymer/gas interfacial tension between polymer melt (**Equation 5**) and especially the supersaturation pressure degree defined as (P_{eq} – P). In this respect, the nuclei concentration as a function of time in a die consequently depends on the variation of pressure over the time. Numerous studies also highlight that the pressure drop rate plays a key role on the amount of nuclei produced during extrusion foaming and *in fine* on the cell density (Park et al. 1995). For this purpose, rheological data was fitted by a Carreau-Yasuda coupled to Arrhenius model (**Equation 6**), and then implemented into the finite element Comsol Multiphysics® software package to compute the pressure-velocity-temperature profile within the die.

$$J = N\left(\frac{2\sigma}{\pi m}\right)^{1/2} exp\left(\frac{-16\pi\sigma^3}{3kT(P_{eq}-P)^2}\right) \textbf{(Eq.5)}$$

with J the nucleation rate (cells/s), N, volume concentration of gas molecules (mol/cm^3), σ the polymer/gas interfacial tension (N.m), m the mass of a gas molecule (kg), K the Boltzmann constant (1.38.10^{-23} kg.s/K), T the melt temperature (K) and (P_{eq} – P) the supersaturation pressure (Pa).

$$\eta(T,\dot{\gamma}) = \eta_0 \exp\,(i_A \times T)(1 + \lambda + \dot{\gamma}^a)^{\frac{m-1}{a}} \textbf{(Eq.6)}$$

with λ the relaxation time (s), m pseudoplasticity index, η_0 the newtonian viscosity (Pa.) and i_A the Arrhenius index (a=2).

Figure 3 (left) displays the evolution of pressure as a function of the distance from the die entrance for PE1 and PE2. In a first approach, the pressure is higher for PE2 than PE1 and this effect is largely attributed to the higher viscosity. Three zones are observed with distinct pressure drops. The first two zones (from x = 0 to 13 mm and from x = 13 to 22 mm) correspond to the entrance of the die where the tube diameter is high and constant, followed by a progressive reduction. Then, the last zone represents the final contraction just before the die exit. This last zone presents the highest pressure drop rate and, based on previous theories on homogeneous nucleation, the cell nucleation should theoretically occur within this final zone. In this context, pressure drop rate were extracted from numerical simulations based on the linear decrease of pressure and the simulated polymer melt velocity.

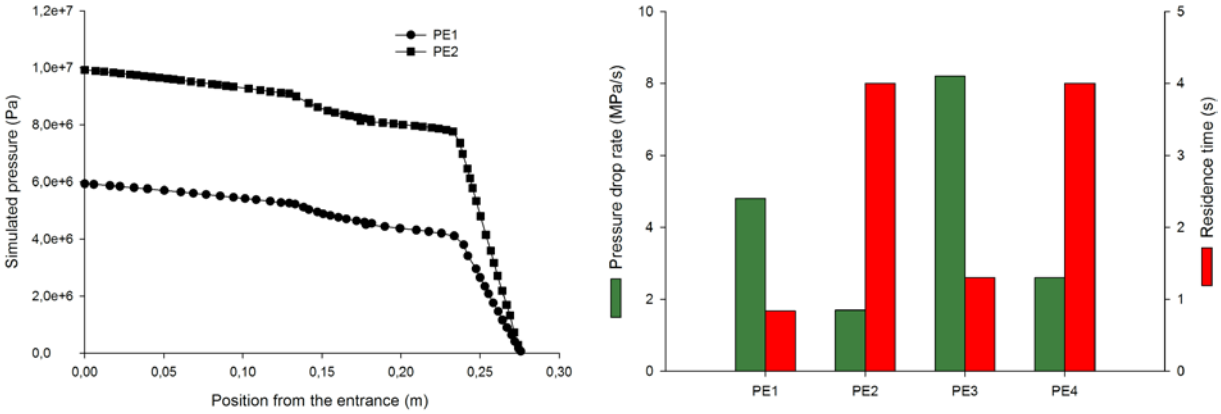

Figure 3: Simulated pressure profiles within the die (left) and simulated pressure drop rate/residence time in the last section of the die for all PE (right).

Figure 3 (right) represents the pressure drop rate for all PEs with values ranging from 2 to 8 MPa/s. Actually, PE could be classified as follows depending on pressure drop rate: PE3 > PE1 > PE2 = P4. However, this classification is in apparent contradiction with classical nucleation theories, since pressure drop rate should theoretically have a positive impact on nucleation rate and *in fine* the cell density (**Table 1**) (Park et al. 1995). The nuclei concentration

is governed by the nucleation rate, but the residence time in the die also affects the cell concentration. In this context, the residence time in the final zone was evaluated from the velocity profile. Residence times ranging from 0.8 to 4 s are obtained and, here, a good correlation is found with the cell density. In this respect, in the present extrusion conditions, high-viscosity polymers favor the nucleation of cell due to enhanced residence time in the die. This effect is mainly ascribed to the low pressure drop rate developed in this die. Indeed, several authors reported pressure drop rate in GPa/s range (approx. 3 decades higher than the present experiments) with cell density higher than10^9 cells/cm^3. Consequently, in the as-presented process, the effect of pressure drop rate is scarce with moderate cell density and the residence time has a powerful influence.

Above-mentioned results were finally extrapolated to biobased PBS. Two commercially-available PBS were chosen with MFI close to 4 – 10 (g/min at 190°C, 2.16 kg). **Figure 4** shows the cross-sectional morphology of cylindrical samples. PBS2 clearly presents uncontrolled foam morphology with heterogeneous large cells. For PBS1, the foam morphology appears more homogeneous with a volume average cell diameter size close to 500 µm and a cell density close to 4.10^5 cells/cm^3. Interestingly, the morphology of PBS1 is similar to that of the low-density poly(ethylene) PE1, but the cell size dispersity appears high (I_D 2.1). Slight modifications of the macromolecular architectures could make sense to get a better control of the cell size. However, strong modifications of the PBS viscosity are required to significantly increase the cell density of PBS foams.

PBS1 and PBS2 were also characterized by dynamic rheology in order to feed numerical simulations with rheological parameters. In terms of pressure drop rate and residence time, only slight differences are observed between PBS1 and PBS2. Thus, the observed differences between the morphologies of PBS foams probably arise from a poor PBS crystallization rate. This hypothesis was checked using calorimetry, and PBS1 displays a significant shift of the crystallization temperature from the melt state by 10°C compared to PBS2. Here again, modifications of the PBS macromolecular architectures could be meaningful to increase crystallization rates.

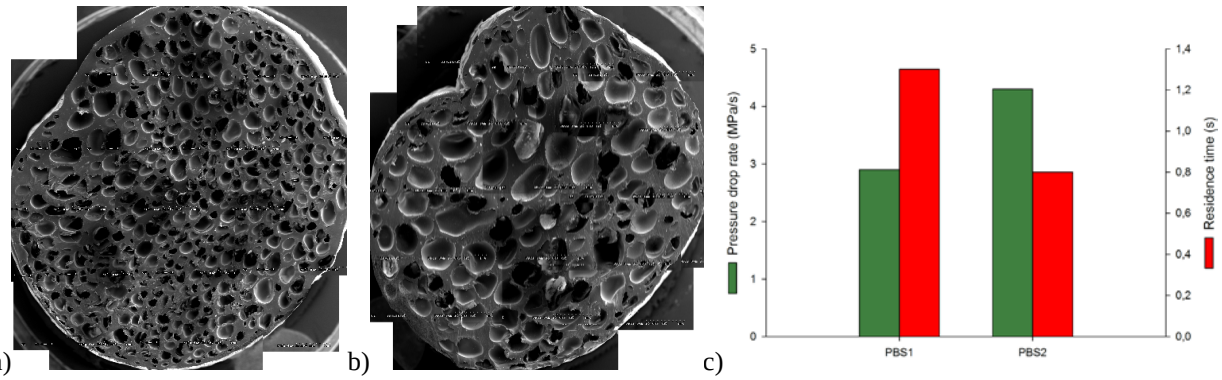

Figure 4: Morphology of PBS1 (a) and PBS2 (b) foams as observed by scanning electron microscopy with subsequent simulated pressure drop rate/residence time profiles (c).

CONCLUSIONS

PE and PBS foams were successfully produced by single-screw extrusion using an endothermic blowing agent. The influence of melt rheology on foam morphology was clarified with various grades of PE with a special emphasis on the effect of the macromolecular architectures. Cell size and cell density could be efficiently tuned by the melt viscosity. Low-viscosity polymers tend to induce large cells with a lower density, whereas high-viscosity ones have the opposite effect. In terms of cell size uniformity, linear polymers should be avoided and branched architectures with viscosity strain-hardening in extensional flows favor a good control of the cell size. PBS foams were also produced with morphologies close to low-viscosity PE. An accurate tuning of PBS foam morphology is currently still difficult, and further developments will therefore focus on the modification of PBS macromolecular architectures to reach higher cell density. Finally, numerical simulations indicated that cell nucleation probably occurs in the final zone of the die and, in the as-reported extrusion conditions, a high influence of the residence time is observed. The pressure drop rate remains low with the chosen die geometry and future experiments will be performed to reach higher pressure drop rate.

ACKNOWLEDGMENT

This project (IFMAS P3A2) has been granted by the French State under the "Programme d'Investissements d'Avenir" Program (contract n°ANR-10-IEED-0004-01) and supported by the French Institute for Biobased Materials (IFMAS, France). The authors thank H. Amedro and S. Marcille (Roquette, France) for their support, and gratefully acknowledge both the International Campus on Safety and Intermodality in Transportation (CISIT, France), the Nord-Pas-de-Calais Region (France) and the European Community (FEDER funds) for their contributions to funding the dynamic rheometer, as well as the Nord-Pas-de-Calais Region (France) for co-funding with IFMAS C. Duborper's PhD grant (contract n°15000305).

REFERENCES

Chaur-Kie L, Shu-Hwang C, Horng-Yith L, Chieh-Chih, T. ANTEC 2005. Boston, USA, 1st-5th May 2005, PDF 102538 CDROM 012
Müller N, Ehrenstein GW, ANTEC 2005, Boston, USA, 1st-5th May 2005, PDF 101625, CD-ROM, 012
Lee J J, Cha S W, Cellular Polymers, 24, 279-297 (2005)
Gomes M.E., Ribeiro A.S., Malafaya P.B., Reis R.L., Cunha A.M., Biomaterials, 22, 883-889 (2001)
Okolieocha C., Raps D., Subramaniam K, Altstädt V,European Polymer Journal, 73, 500-519 (2015)
Stralen SJD, International Journal of Heat and Mass Transfer, 9, 995–1020 (1966)
Lee ST, Park CB, Ramesh NS, Polymeric foams : Science and Technology. 2007
Wang G, Guo B, Li R., Journal of Applied Polymer Science, 124, 1271-1280 (2011)
Julien JM , Quantin JC; Benezet JC ; Bergeret A; Lacrampe MF, Krawczak P, Polymer, 53, 5885-5895, 2012
Julien JM ; Benezet, Lafranche, Quantin JC; Bergeret A; Lacrampe MF; Krawczak, P, European Polymer Journal, 67, 40-49 (2015)
Willett JL; Shogren RL, Polymer, 43, 5935-5947 (2002)
Spitael P; Macosko CW, Polymer Engineering & Science, 44, 2090–2100, (2004)
Park CB; Baldwin DF; Suh NP, Polymer Engineering & Science, 35, 432–440, (1995)